Korean J. of Chem. Eng., 11(3), 204-210 (1994)

BUBBLE PROPERTIES AND PRESSURE FLUCTUATIONS IN BUBBLE COLUMNS

Hyeuk Woong Kwon, Joo Hee Han, Yong Kang* and Sang Done Kim†

Dept. of Chem. Eng., Korea Advanced Institute of Science and Technology, Taejon 305-701, Korea
*Dept. of Chem. Eng., Chungnam National University, Taejon 305-764, Korea
(Received 20 January 1994 • accepted 4 March 1994)

Abstract—The effects of gas (0.02-0.1 m/s) and liquid velocities (0.0-0.10 m/s) on the bubble properties and pressure fluctuations have been determined in a 0.376 m-ID×2.1 m-high bubble column. The pressure fluctuations have been analyzed by resorting to the Fractal analysis; the time series of pressure fluctuation signals have been analyzed by means of the Rescaled range analysis and the Hurst exponent has been obtained. The bubble chord length and its rising velocity increase but the Hurst exponent decreases with increasing gas velocity. Whereas, the bubble chord length decreases, but the Hurst exponent increases with an increase in liquid velocity in the continuous bubble column (U_L>0.02 m/s). The Hurst exponent has been found to have a definite relationship with the bubble chord length and its standard deviation.

INTRODUCTION

Bubble columns have been found in numerous industrial applications as reactors, contactors and separation units in the chemical, mining, pharmaceutical and biochemical industries, since they have exhibited high heat and mass transfer rates due to efficient contact between the phases during continuous operation [1-3].

The bubble column generally comprises gas bubbles as a dispersed in the upward continuous flowing liquid phase. Thus, the motion and flow behavior of gas bubbles have been recognized as the fatal elements to determine the hydrodynamic characteristics of bubble columns. Therefore, several investigators [4-9] have examined the bubble properties and its flow behavior in bubble columns however, the effects of bubble properties on the performance of bubble column reactors or contactors are not well defined until now since the bubbling phenomena in the bubble columns are extremely complex. Thus, the fault diagnosis of the bubble column system, pressure fluctuations in the system can be used as the diagnostic tools for the detection of the highly stochastic and random bubbling motions in the system.

Recently, the pressure fluctuation signals from the multiphase flow systems have been successfully analyzed by means of the Rescaled range analysis [10-13], which is based on the concept of fractional Brownian motion [14].

In the present study, the bubbling phenomena in bubble columns have been investigated by means of the Fractal analysis; the time series of the pressure fluctuation signals have been analyzed by resorting to the Rescaled range analysis. The relationships between bubble property (chord length, rising velocity) and the pressure fluctuations have been determine in bubble columns.

THEORY

The model of fractional Brownian motion (FBM) has been proposed by Mandelbrot and van Ness [14] from the central concept of Brownian motion; it is one of the major contributions in the field of temporal fractals. FBM [$B_H(t)$] is a single-valued function of one variable, t (usually time), which is capable of identifying and interpreting long-term persistence or correlation in a time series. A sequence of the increments of FBM (i.e., [$B_H(t_1)-B_H(t_0)$]) has the scaling property which is characterized by parameter, H, in the range, $0<H<1$, with the simple relation of $B_H(t_1)-B_H(t_0)\propto(t_1-t_0)^H$. The increment, [$B_H(t+\tau)-B_H(t)$], of FBM yields a Gaussian distribution with a variance proportional to τ^{2H}. For the classical Brownian motion, $H=1/2$ and thus its variance is proportional to τ^H.

†To whom all correspondences to be addressed.

It is well known that the FBM, $B_H(t)$, has a long run correlation; for $H>1/2$, the increments of $B_H(t)$ are positively correlated for all values of t whereas, for $H<1/2$, the increments negatively correlated for all values of t. The former is called "persistence" and the latter is called "antipersistence". In case of $H=1/2$, the sequence of increments corresponds to the independent increment process of the classical Brownian motion, i.e. the correlation vanishes [10, 11]. The record of antipersistent process appears very noisy, i.e. the local noise is the same order of magnitude as the total excursions of the record. A persistent process exhibit rather clear trends with relatively little noise [15].

1. Construction of the Sample Range

To obtain H for a given pressure fluctuation, the sample and rescaled ranges have to be defined and constructed as follows [10-12].

For a given time series of the recorded pressure fluctuations, X(t), spaced in time (t) from 1 to T, the mean value of the recorded signals within subrecord from time $t+1$ to time $t+\tau$ can be written as

$$\frac{1}{\tau}\left[X^*(t+\tau)-X^*(t)\right] \tag{1}$$

where $X^*(t)$ is defined as

$$X^*(t)=\sum_{u=1}^{t} X(u) \tag{2}$$

Here, let B(t, u) denotes the cumulative departure of $X(t+u)$ from the mean value for the subrecord between time $t+1$ to time $t+\tau$ as can be written as

$$B(t,u)=\left[X^*(t+u)-X^*(t)\right]-\left(\frac{u}{\tau}\right)\left[X^*(t+\tau)-X^*(t)\right] \tag{3}$$

Then, the sample sequential range, $R(t,\tau)$ can be defined as

$$R(t,\tau)=\underset{0\le u\le\tau}{\text{Max.}}\ B(t,u)-\underset{0\le u\le\tau}{\text{Min.}}\ B(t,u) \tag{4}$$

On the other hand, the sample sequential variance of the subrecord from time $t+1$ to time $t+\tau$ can be written as

$$S^2(t,\tau)=\frac{1}{\tau}\sum_{u=t+1}^{t+\tau} X^2(u)-\left[\frac{1}{t}\sum_{u=t+1}^{t+\tau} X(u)\right]^2 \tag{5}$$

Thus, the ratio of $R(t,\tau)/S(t,\tau)$ can be obtained which is termed as the rescaled range. As can be written in Eq. (6), the R/S ratio has been found to scale as a power function of τ;

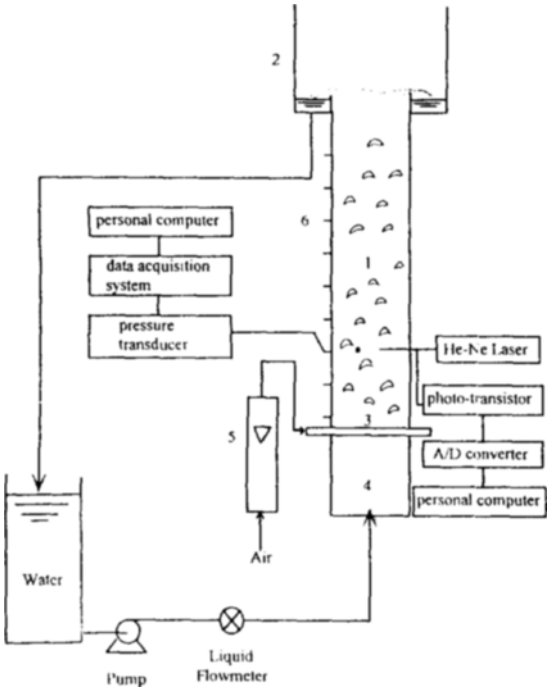

Fig. 1. Schematic diagram of the experimental apparatus.

1. Main column
2. Weir
3. Distributor
4. Calming section
5. Gas rotameter
6. Pressure taps

$$\frac{R(t,\tau)}{S(t,\tau)}\propto\tau^H \tag{6}$$

where H is the Hurst exponent.

Where R/S ratio scales as τ^H where $H>1/2$, it is long-term persistence or correlation, often called "Hurst Phenomenon" [15].

EXPERIMENTAL

Experiments were carried out in a 0.376 m-ID×2.1 m-high Plexiglas column as shown in Fig. 1. A perforated plate which contained 786 evenly spaced holes (3 mm-ID) which served as a liquid distributor. Air was fed to the column through 6.4 mm perforated feed pipes with 232 holes of 1.0 mm-ID drilled horizontally through the grid. Pressure taps were mounted flush with the column wall at 0.14 m height intervals. The static pressure at each point was measured by a liquid manometer. Water and oil-free compressed air was used as a liquid and a gas phase, respectively.

1. Pressure Fluctuation

The pressure tap was located at 0.4 m from the distributor. One of two channels of the differental pressure transducer was connected to the pressure tap. The remaining channel was pressurized by the water column having static head equivalent to the mean static pressure in the column; the transducer yielded pressure fluctuations. The pressure transducer produced an output voltage proportional to the pressure fluctuations. Signals were processed with the aid of data acquisition system (Data Precision Model, D-6000) and a personal computer (IBM-AT 486). The pressure fluctuation signals, which is a voltage-time signal corresponding to the pressure-time signal, were sampled through the data acquisition system with the sampling rate of 0.01 s and transferred to the personal computer. A total acquisition was 40 s and a typical sample comprised 4000 points. This combination of sampling rate and length ensured that the full spectrum of hydrodynamic signals, typically 0-25 Hz, was captured from the bubble column.

2. Bubble Chord Length

The bubble chord length and its rising velocity were measured by means of a two-channel optical fiber probe which was made of a plastic fiber of 0.250 mm in diameter. The probe was made by bending the fiber into a U-shape and encasing the entire fiber except the U-shaped bend in a stainless-steel tube of 6.0 mm diameter [4, 9]. The distance between the two tips was 2.0 mm. The probe was located at 0.40 m from the distributor and its radial positions were either 0.0, 0.16, 0.32, 0.48, 0.64, or 0.80 in dimensionless radial direction (r/R). A He-Ne laser was used as the light source and two photo transistors were used as converters of light intensity to electrical voltage. The signals were fed to the personal computer at the selected sampling rate of 500 μs. The sampling time was 90 s and the total number of measured bubble during the sampling time was in the range of 100-400. The mean bubble chord length, $l_{v,mean}$, was calculated by Eq. (7) as the follow

$$l_{v,mean}=\frac{\sum_{r/R=0}^{0.8}(N_{b,r/R})(l_{v,r/R})}{\sum_{r/R=0}^{0.8}N_{b,r/R}} \tag{7}$$

where $N_{b,r/R}$ is the number of ascending bubbles and $l_{v,r/R}$ is the bubble chord length detected at the radial position, r/R, respectively. Details of data processing on the bubble properties is described else where [9].

RESULTS AND DISCUSSION

1. Bubble Properties

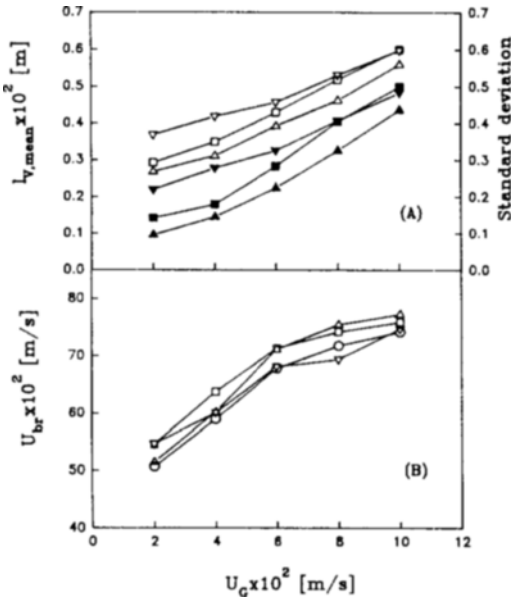

Fig. 2. Effects of U_G on l_v, it's standard deviation and U_{br} in bubble columns (filled symbol for the standard deviation of l_v).

	○	▽	□	△	▼	■	▲
$U_L\times10^2$ [m/s]	0.0	4.0	6.0	10.0	4.0	6.0	10.0

The effect of gas velocity on the bubble chord length, its standard deviation, and bubble rising velocity in bubble columns is shown in Fig. 2, where all of these bubble properties increase with an increase in gas velocity since the probability of bubble coalescence can increase as a result of the increase in the bubble density in the column with increasing gas velocity. Prince and Blanch [5] reported that bubble coalescence can be modeled by considering the bubble collisions due to turbulence, buoyancy, and laminar shear, and that bubble break-up can be analyzed in terms of bubble interactions whith turbulent eddies. They also suggested that the bubble collisions might result from the random motion of bubbles due to turbulence and different rising velcoity of bubbles owing to different size. Anyhow, bubbles located in a region of relatively high liquid velocity may collide with bubbles in a slower section of the velocity field. Thus, the bubble coalescence would occur irregularly, which leads to the non-uniform distribution of bubble size in the bed. These can explain the reason why the standard deviation of the bubble length increases with an increase in gas velocity (Fig. 2A).

The bubble coalescence can produce the larger bubbles and increase their rising velocity since bubble

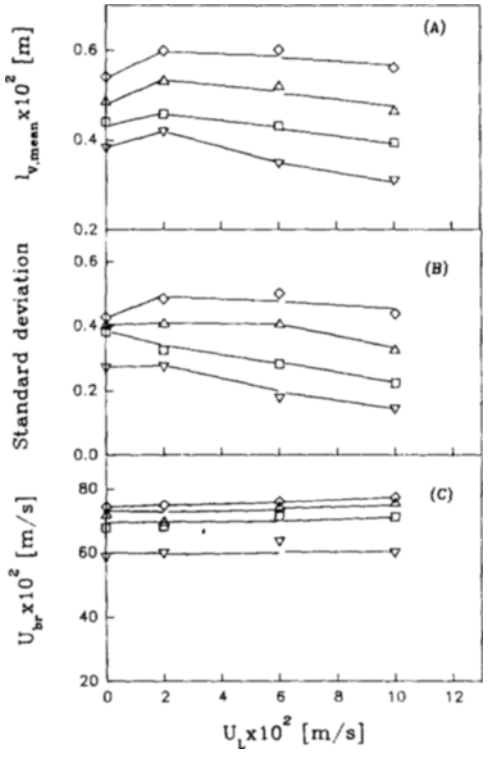

Fig. 3. Effects of U_L on l, and it's standard deviation and U_{br} in bubble columns.

	▽	□	△	◇
$U_G \times 10^2$ [m/s]	4.0	6.0	8.0	10.0

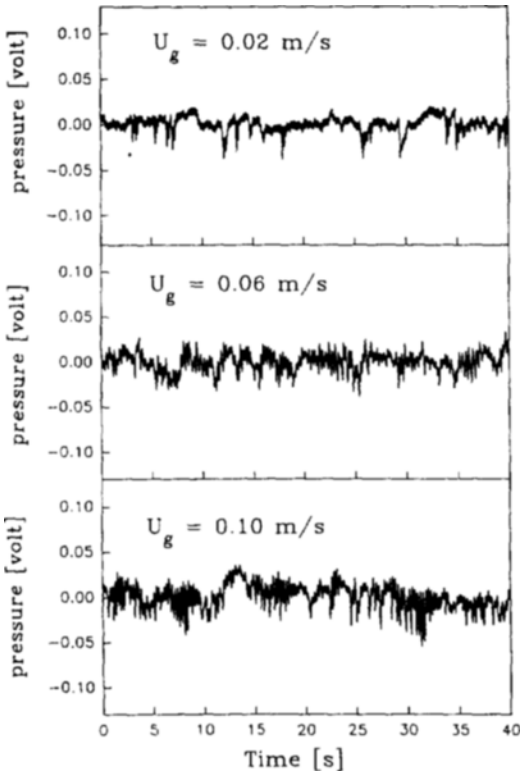

Fig. 4. Typical examples of pressure fluctuation signals in bubble columns (U_L=0.10 m/s).

rising velocity is proportional to the bubble size in the column [4]. As can be seen in Fig. 2B, the rate of increase in bubble rising velocity decreases with increasing gas velocity. This trend can be anticipated from the increase of hindrance effect between the adjacent bubble swarms with increasing gas velocity [2, 6].

The effect of liquid velocity on bubble properties in bubble columns is shown in Fig. 3. As can be seen in Fig. 3A, the bubble chord length exhibits the slight maximum with an increase in liquid velocity however, it decreases almost linearly with the liquid velocity in the range of $0.02<U_L<0.10$ m/s. Not that the increase in the fluid element velocity of the continuous liquid phase can enhance the turbulence intensity and the bubble rising velocity in the multiphase system [16]. The increase of turbulence can let the bubbles become unstable, and the increase of bubble rising velocity can reduce the probability and time of bubble coalescence in the column, thus, these consequently lead to the reduction of bubble chord length with increasing liquid velocity as found previous studies in 0.254 m-ID and 0.152 m-ID bubble columns [4, 9]. However, the bubble chord length increases slightly by introducing the liquid to the static bubble column (U_L=0.0 m/s), because the bubble size reduction by turbulence intensity may be overcome by the increase of probability of bubble collision due to the increase of fluctuation of velocity profiles at the relatively lower liquid velocity ranges ($U_L<0.02$ m/s).

As can be seen in Fig. 3C, the effect of liquid velocity on bubble rising velocity is negligible. Whereas, the bubbles can be disintegrated by the small-scale liquid eddies, they are also dragged along by the liquid flow, with an increase in liquid velocity. Therefore, the bubble rising velocity is not changed considerably with the liquid velocity since the above two effects may compensate each other [8].

2. Pressure Fluctuations

Typical time series of pressure fluctuation signals from bubble can be seen in Fig. 4 with the variation of gas velocity. As can be seen, the amplitude and frequency of pressure fluctuation signals increase with

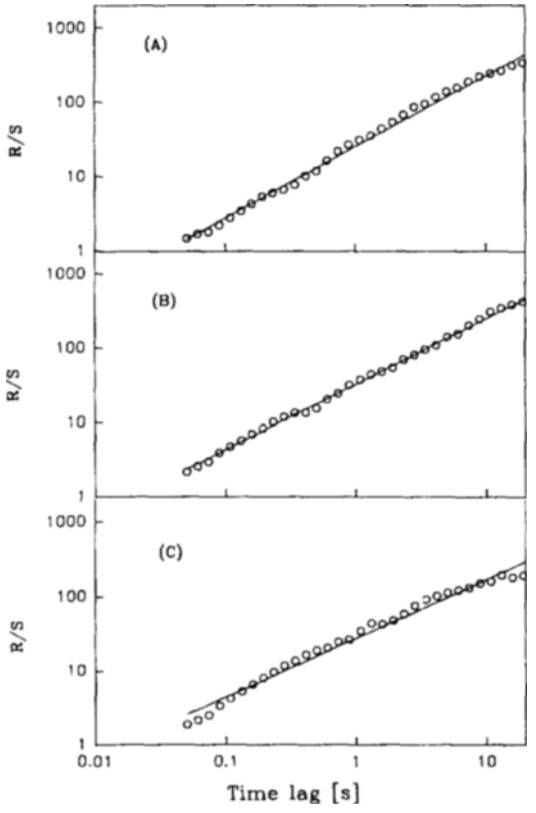

Fig. 5. Typical Pox diagram for pressure fluctuation signals in bubble columns.

	(A)	(B)	(C)
$U_L \times 10^2$ [m/s]	10.0	2.0	2.0
$U_G \times 10^2$ [m/s]	2.0	2.0	10.0
H(-)	0.96	0.87	0.79

increasing gas velocity due to the increase in the size and frequency of the rising bubbles.

The rescaled range of the data has been correlated with the time lag as shown in Fig. 5. The value of the Hurst exponent (H) has been determined from the slope of the plot with the correlation coefficients higher than 0.98 in the entire operating range employed in this study.

The variation of the Hurst exponent (H) with variation of gas velocity in bubble columns is shown in Fig. 6, where the H decreases gradually with an increase in gas velocity. As can be seen, the pressure fluctuation signals become less persistent with an increase in gas velocity [13]. In other words, the system becomes more random and less predictable owing to the complex contacting of multiphase with an increase in gas velocity. The inner structure of bubble columns

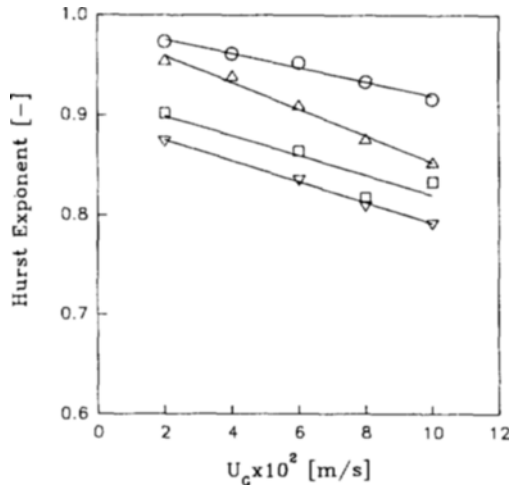

Fig. 6. Effect of U_G on H in bubble columns.

	○	▽	□	△
$U_L \times 10^2$ [m/s]	0.0	2.0	6.0	10.0

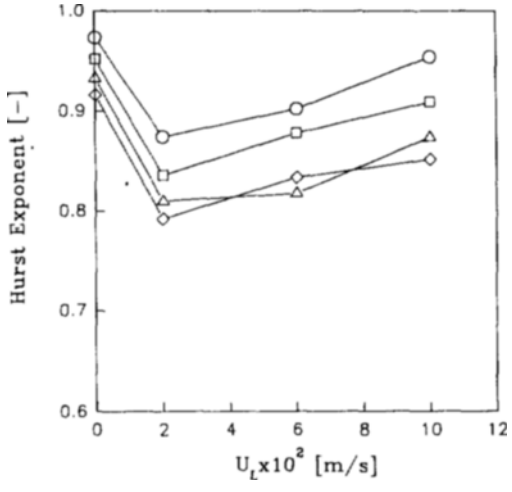

Fig. 7. Effects of U_L on H in bubble columns.

	○	□	△	▽
$U_G \times 10^2$ [m/s]	2.0	6.0	8.0	10.0

has been known to depend on the contacting and flow modes of the dispersed phase such as rising bubbles [6].

The amount of gas bubble as a dispersed phase in the system increases with increasing gas velocity. With increasing gas velocity, the frequency of bubble contacting and coalescence as well as the turbulence intensity increase [4, 5, 9, 16]. The bubble coalescence can produce the larger bubbles having higher rising velocity since bubble rising velocity is proportional to the

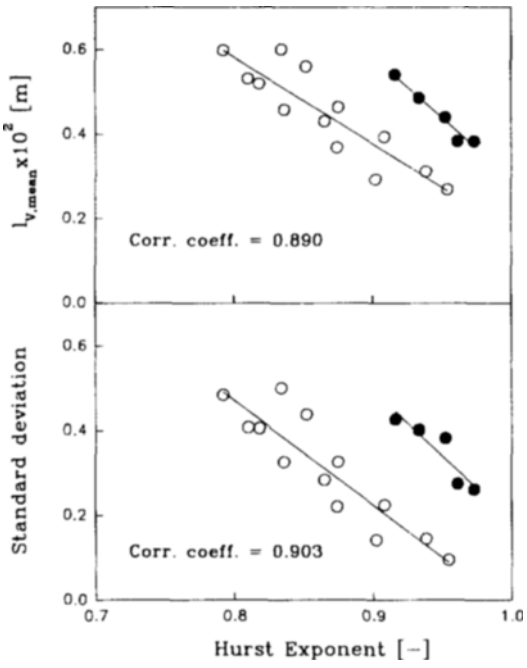

Fig. 8. Relationship between H and bubble properties (○: U_L>0.02 m/s, ●: U_L=0.0 m/s).

bubble size in the column [4, 9]. However, the probability of bubble coalescence is stochastically nonuniform throughout the column. Therefore, bubble size and its rising velocity are distributed widely thus, the pressure fluctuation signals generated from this nonuniform bubble flow condition are less persistent, and the standard deviation of bubble size becomes significant with increasing gas velocity.

The effect of liquid velocity on the Hurst exponent (H) can be seen in Fig. 7 where the H exhibits the minimum value with an increase in liquid velocity. This trend can be anticipated from Fig. 3A that the bubble chord length increases with introducing the liquid to the static bubble column but it decreases almost linearly with an increase in liquid velocity higher than 0.02 m/s, since the pressure fluctuations strongly depend on the bubble size in the bubble column. In the multiphase flow systems, the influences of dispersed phase flow on the hydrodynamics have become remarkable with an increase in bubble size.

For the optimal control and fault diagnosis of the bubble column system, it is essential to analyze the bubbling phenomena in the column during the system is operating. Therefore, it is a valuable means to estimate the bubble chord length from the Hurst exponent which can be determined immediately from the pressure fluctuation signals during the operation of the system. As can be seen in Fig. 8, a definite relationship can be obtained found between the bubble chord length and the Hurst exponent. Note that the bubble chord length generally decreases with increasing the Hurst exponent, which represents the system becomes more stable with the smaller bubble size.

CONCLUSIONS

The bubbling phenomena in bubble columns have been analyzed by means of the rescaled range analysis of pressure fluctuations from which the Hurst exponent can be estimated.

The bubble chord length and its rising velocity increase but Hurst exponent decrease with an increase in gas velocity. Whereas, the bubble chord length exhibits the maximum value but Hurst exponent shows the minimum value with an increase in liquid velocity in the bubble. However, the bubble chord length decreases almost linearly but Hurst exponent increases linearly with an increase in liquid velocity higher than 0.02 m/s. The effect of liquid velocity on bubble rising velocity is found to be insignificant. The Hurst exponents have a definite relationship with the bubble chord length and its standard deviation.

NOMENCLATURE

d_p : particle diameter [m]
D_T : column diameter [m]
H : Hurst exponent [-]
$l_{v,mean}$: mean bubble chord length [m]
r : radial position from center [m]
R : column radius [m]
R(t, τ) : sample sequential range for lag τ
$S^2(t, \tau)$: variance
t : time [s]
T : total available sample size
U_{br} : bubble rising velocity [m/s]
U_L : liquid superficial velocity [m/s]
U_G : gas superficial velocity [m/s]
X(t) : time series

Greek Letter

τ : time-lag [s]

REFERENCES

1. Shah, Y. T., Kelkar, B. G., Godbole, S. P. and Deckwer, W. D.: *AIChE J.*, **28**, 353 (1982).
2. Deckwer, W. D. and Shumpe, A.: *Int. Chem. Eng.*,

27, 405 (1987).
3. Kim, S. D. and Chang, H. S.: *Hwahak Konghak*, **17**, 407 (1979).
4. Yu, Y. H. and Kim, S. D.: *Chem. Eng. Sci.*, **46**, 313 (1991).
5. Prince, M. J. and Blanch, H. W.: *AIChE J.*, **36**, 1485 (1990).
6. Kang, Y., Lim, W. M. and Kim, S. D.: *Hwahak Konghak*, **25**, 460 (1987).
7. Ueyama, K. and Miyauchi, T.: *AIChE J.*, **25**, 258 (1979).
8. Teital, Y. D., Borneam, D. and Dukler, A. E.: *AIChE J.*, **26**, 345 (1980).
9. Han, J. H.: "Hydrodynamic Characteristics of Three Phase Fluidized Beds", Ph.D. Thesis, KAIST (1990).
10. Fan, L. T., Neogi, D., Yashima, M. and Nassar, R.: *AIChE J.*, **36**, 1529 (1990).
11. Fan, L. T., Kang, Y., Neogi, D. and Yashima, M.: *AIChE J.*, **39**, 513 (1993).
12. Kang, Y., Min, B. T., Kim, S. D., Yashima, M. and Fan. L. T.: Proc. 23rd Annual Meeting of the Fine Particle Society, Las Vegas, Nevada 1992.
13. Drahos, J., Bradka, F. and Puncochar, M.: *Chem. Eng. Sci.*, **47**, 4067 (1992).
14. Mandelbrot, B. B. and van Ness, J. W.: *SIAM Rev.*, **10**, 422 (1968).
15. Feder, J.: "Fractals", Plenum Press, New York (1988).
16. Kang, Y. and Kim, S. D.: *Ind. Eng. Chem. Process Des. Dev.*, **25**, 717 (1986).